Theor. Comput. Fluid Dyn. (2010) 24:137–149
DOI 10.1007/s00162-009-0109-6

ORIGINAL ARTICLE

Paul K. Newton

The *N*-vortex problem on a sphere: geophysical mechanisms that break integrability

Received: 4 November 2008 / Accepted: 31 March 2009 / Published online: 7 June 2009

Abstract We describe the dynamical system governing the evolution of a system of point vortices on a rotating spherical shell, highlighting features which break what would otherwise be an integrable problem. The importance of the misalignment of the center-of-vorticity vector associated with a cluster of point vortices with the axis of rotation is emphasized as a crucial factor in the interpretation of dynamical features for many flow configurations. We then describe two important physical mechanisms which break what would otherwise be an integrable problem—the interactions between the local center-of-vorticity vectors of more than one region of concentrated vorticity, and the coupling between the center-of-vorticity vector and the background vorticity field which supports Rossby waves. Focusing on the Polar vortex splitting event of September 2002, we describe simple (i.e., low dimensional) mechanisms that can trigger instabilities whose subsequent development cause the onset of chaotic advection and global particle transport. At the linear level, eigenvalues that oscillate between elliptic and hyperbolic configurations initiate the pinch-off process of a passive patch representing the Polar vortex. At the nonlinear level, the evolution and topological bifurcations of the streamline patterns are responsible for its further splitting, stretching, and subsequent transport over the sphere. We finish by briefly describing how to incorporate conservation of potential vorticity and the development of a model governing the probability density function associated with the point vortex system.

Keywords *N*-vortex problem on sphere · Nonintegrable Hamiltonian systems · Antarctic polar vortex

PACS 47.32.C-, 47.10.Fg, 45.50.Jf, 92.60.-e

1 Introduction and derivation of equations

In this article, we describe models based on point vortex discretizations of the vorticity field for incompressible flow on a sphere. Our context is the modeling of atmospheric events and our primary focus is on identifying physical mechanisms that complicate the clean, integrable aspects of the core problem, which is now well understood and whose literature can be found in Newton [23]. This paper summarizes the author's Keynote lecture presented at the IUTAM Symposium '150 Years of Vortex Dynamics' which took place at the Danish Technical University, Copenhagen, 12–16 Oct 2008. In the paper, I attempt to: (i) set the stage for the geophysical context for the models presented; (ii) summarize and review a coherent theme developed in recent papers by the author and co-workers; (iii) highlight where and how the types of low-dimensional discrete vortex models presented are useful in gaining insights into how much more complex geophysical processes 'break-integrability'; (iv) point to important extensions of the current hierarchy of models that are key towards making the models more useful with respect to understanding atmospheric flows.

Communicated by H. Aref

P. K. Newton
University of Southern California, Los Angeles, USA
E-mail: newton@usc.edu; newton5@cox.net

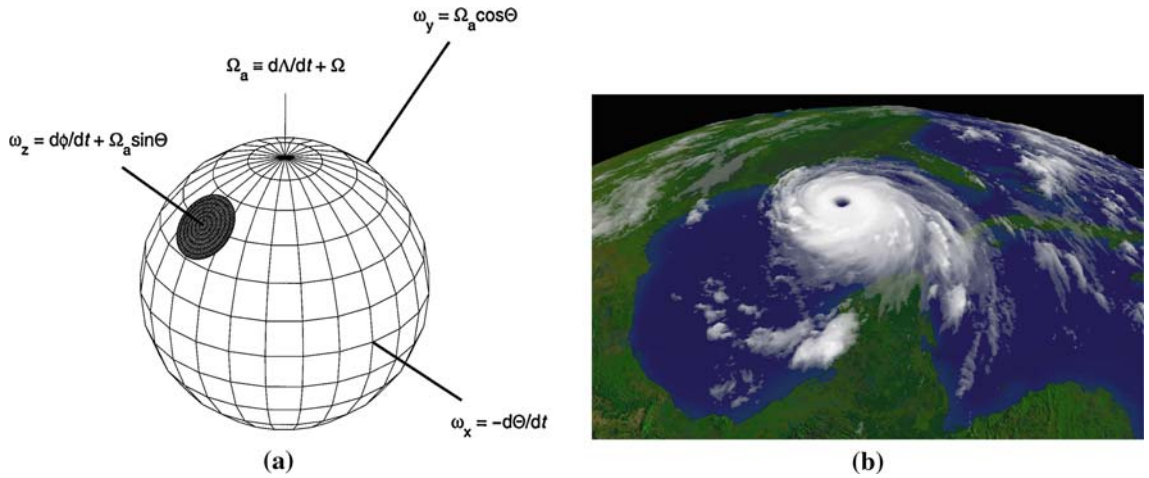

Fig. 1 **a** A (frictionless) spinning disc on a rotating sphere has been studied as a simple mechanistic model of a geophysical vortex. Original figure can be found in Ripa [33]. **b** Yet even the most highly concentrated vorticity fields (Hurricane Katrina 23 August 2005) present additional modeling complications due to internal deformations, filamentation, background coupling, and vertical stratification (http://www.nnvl.noaa.gov/)

To set the stage, we mention recent work on the modeling and dynamics of a frictionless spinning disc on the surface of a rotating sphere, as shown in Fig. 1a, which presents a clean barebones model of some of the key features encountered when attempting to model the evolution of a concentrated geophysical vortex on a rotating planet. The initial work of Nycander [28] established the analogy between the steady westward drift of a distributed geophysical vortex and the steady precession of a rigid body. This was followed by McDonald [21] who further pointed out that the nutation of a rigid body is analogous to unsteady inertial oscillations of geophysical vortex trajectories. Then Ripa [32–34] systematically compared the errors due to a β-plane treatment as opposed to a full spherical approach, documenting the subsequent errors on the order $O(R^{-1})$, where R is the earth's radius. From this work, it is clear that even the most highly concentrated vorticity field on the sphere, such as Hurricane Katrina, shown in Fig. 1b, presents significant additional modeling challenges due to the distributed vorticity fields associated with hurricanes, as well as the additional 'background' vorticity field spread across the spherical surface with which it interacts. In addition, traditional β-plane models, while unquestionably useful, do not paint a complete picture of the kinds of dynamical and kinematic mechanisms that can occur on the full sphere.

Two of the main features we emphasize in this paper are (i) the nonlinear coupling between distinct concentrated clusters of vorticity, as shown in Fig. 2, and (ii) the nonlinear coupling of these clusters with the background field which supports Rossby waves, as shown in Fig. 3. The first can be modeled staying within the context of finite-dimensional systems ($N < \infty$), while the second requires that the point vortices be placed in a continuous background field and thus be viewed as an 'embedded' dynamical system.

1.1 Interacting particle system

Consider a charged point-particle of strength $\Gamma_\beta \in \mathbb{R}$ located at the North pole on a unit sphere. It generates a velocity field that is independent of the azimuthal coordinate ϕ. Assume its influence decreases like $1/L^2$, where $L = \sqrt{2(1-\cos\theta)}$ is the chord distance, as shown in Fig. 4. This gives rise to a velocity field:

$$\dot{\theta} = 0, \tag{1}$$

$$\dot{\phi} = \frac{\Gamma_\beta}{2\pi}\frac{1}{L^2} = \frac{\Gamma_\beta}{4\pi}\frac{1}{(1-\cos\theta)}. \tag{2}$$

In Cartesian coordinates, with:

$$\mathbf{x}_\beta = (0,0,1); \quad \mathbf{x} = (\sin\theta\cos\phi, \sin\theta\sin\phi, \cos\theta), \tag{3}$$

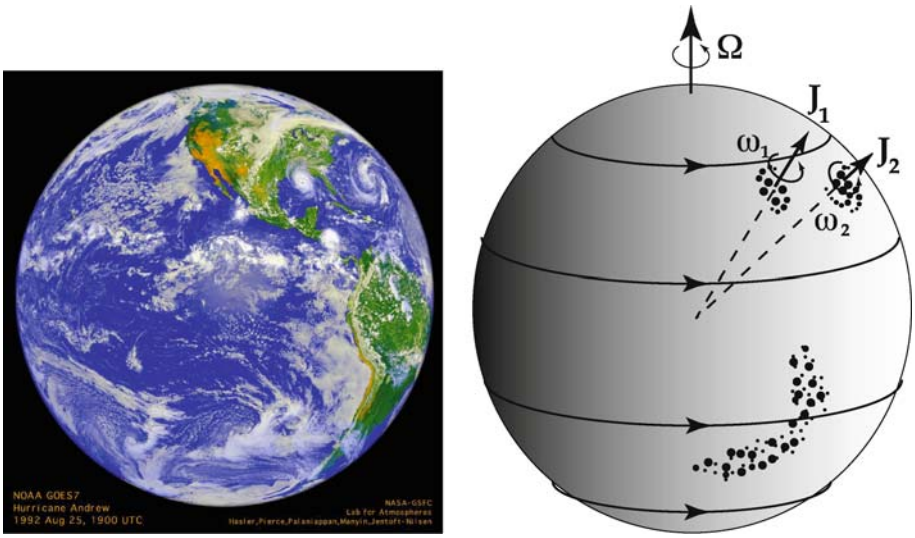

Fig. 2 **a** Satellite photo of Hurricane Andrew (http://jpl.nasa.gov/), a category 5 hurricane formed on 16 August 1992. The cloud formations provide a snapshot of the instantaneous vorticity field (approximate) on a two-dimensional spherical shell. **b** Each concentrated vorticity region has a local center-of-vorticity vector (shown are J_1 and J_2) which is misaligned with the axis of rotation. Also shown is the background field represented as solid-body rotation and distributed point vortices throughout. The embedded dynamical system will evolve from this initial state via a complex evolution involving all of these key ingredients

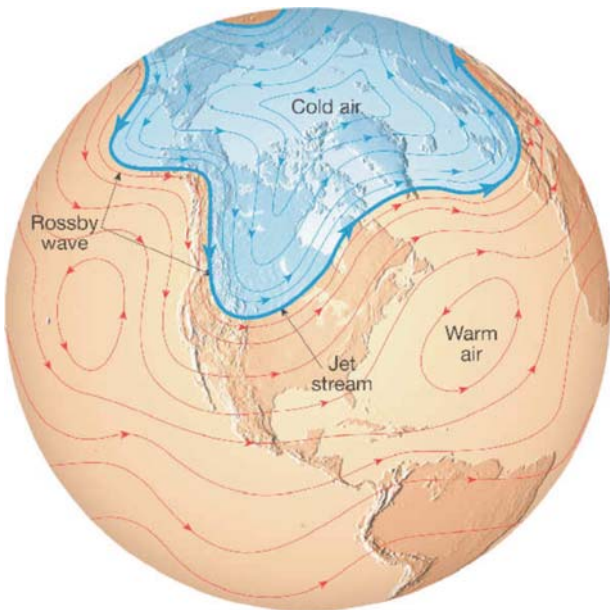

Fig. 3 Rossby waves are the main physical mechanism that couple to the concentrated vorticity clusters and destroy rotational symmetry about the polar axis breaking conserved quantities. Polar and subtropical jetstreams provide symmetry-breaking perturbations to the underlying solid-body velocity field. Download from http://www.daukas.com

it is straightforward to show that (1), (2) are equivalent to

$$\dot{\mathbf{x}} = \frac{\Gamma_\beta}{4\pi} \frac{\mathbf{x}_\beta \times \mathbf{x}}{(1 - \mathbf{x} \cdot \mathbf{x}_\beta)}, \tag{4}$$

$$\mathbf{x}_\beta = (0, 0, 1); \quad \mathbf{x} = (x, y, z); \quad \|\mathbf{x}\| = 1. \tag{5}$$

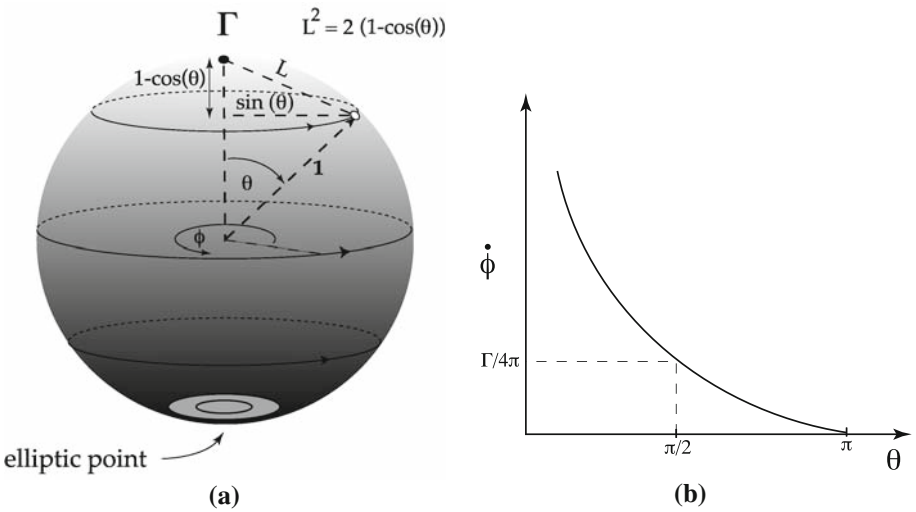

Fig. 4 **a** A particle with strength Γ located at the North Pole generates a velocity field on the sphere which is azimuthally independent (i.e., moves on constant latitudinal curves) and decays with distance. An elliptic fixed point at the antipode is a topological necessity as a result of the Poincaré index theorem. **b** The angular velocity from the North Pole decays monotonically with distance

By linear superposition, a collection of N particles, each with their own strength $\Gamma_\beta \in \mathbb{R}$ $(\beta = 1, \ldots, N)$, generates the velocity field:

$$\dot{\mathbf{x}} = \sum_{\beta=1}^{N} \frac{\Gamma_\beta}{4\pi} \frac{\mathbf{x}_\beta \times \mathbf{x}}{(1 - \mathbf{x} \cdot \mathbf{x}_\beta)}. \tag{6}$$

This equation expresses the velocity on the sphere in terms of the vorticity distribution, which we recognize as a discrete inversion of the vorticity–velocity relation $\omega = \nabla \times \mathbf{u}$. In fact, (6) is the *discrete Biot-Savart law* on the unit sphere [23]. Finally, invoking Helmholtz' [14] assumption that each particle moves with the local fluid velocity, we replace $\mathbf{x}$ with $\mathbf{x}_\alpha$ to obtain the N-vortex dynamical system on the sphere:

$$\dot{\mathbf{x}}_\alpha = \sum_{\beta=1}^{N}{}' \frac{\Gamma_\beta}{4\pi} \frac{\mathbf{x}_\beta \times \mathbf{x}_\alpha}{(1 - \mathbf{x}_\alpha \cdot \mathbf{x}_\beta)}, \quad (\alpha = 1, \ldots, N) \tag{7}$$

$$l_{\alpha\beta}^2 = |\mathbf{x}_\alpha - \mathbf{x}_\beta|^2 = 2(1 - \mathbf{x}_\alpha \cdot \mathbf{x}_\beta). \tag{8}$$

The prime on the summation indicates that we exclude the term $\beta = \alpha$ so as to avoid the singularity. It is worth pointing out that (7) can also be written as:

$$\dot{\mathbf{x}}_\alpha = \sum_{\beta=1}^{N}{}' \frac{\Gamma_\beta}{2\pi} \frac{\hat{\mathbf{n}}_\beta \times (\mathbf{x}_\alpha - \mathbf{x}_\beta)}{l_{\alpha\beta}^2}, \quad (\alpha = 1, \ldots, N) \tag{9}$$

where $\hat{\mathbf{n}}_\beta$ is the unit normal vector on the sphere at the vortex location, i.e., $\hat{\mathbf{n}}_\beta \equiv \mathbf{x}_\beta$. The planar N-vortex equations are obtained from (9) by using the unit normal in the plane, i.e., $\hat{\mathbf{n}}_\beta \equiv \hat{e}_z$. Thus, the spherical problem contains an extra coupling term arising from the unit normal to the surface that the planar problem does not contain, as the normal vector on the plane is constant.

Figure 4 brings out another important difference between the spherical and planar problems. Since the velocity field is invariant to rotations around the North-South polar axis, it is clear that an elliptic fixed point at the South Pole is forced upon us by topological considerations. Thus, if c represents the number of *centers* of the vector field (which in this case is two) and s represents the number of *saddles* (which in this case is zero) then $c - s = 2$. This simple and intuitive fact is a consequence of a much deeper and more general result, known as the *Poincaré index theorem* which states that the index $I_f(S)$ of a two-dimensional surface S relative to any C^1 vector field f on S with at most a finite number of critical points, is equal to the Euler–Poincaré characteristic

of S, denoted $\chi(S)$, i.e., $I_f(S) = \chi(S)$. It is a standard topological fact (see Katok and Hasselblatt [17]) that for a sphere, $\chi(S) = 2$. The index for a center is $+1$, while that for a saddle is -1. Hence, if c denotes the number of centers present (point vortices plus other centers), and s denotes the number of saddles, then one must have $c - s = 2$. These facts were exploited by Kidambi and Newton [19] to categorize all integrable streamline patterns on the sphere. A surprising result is that for $N \leq 3$, there are only 12 topologically distinct 'primitive' patterns, each of which can be homotopically deformed to form a catalogue of 35 kinematically distinct patterns from which all 'snapshots' of an integrable flowfield can be built.

1.2 Spherical coordinates

While the Cartesian formulation is, in some ways the most transparent, for the purposes of studying integrability, the spherical coordinate system is more useful. With

$$\mathbf{x}_\alpha = (\sin\theta_\alpha \cos\phi_\alpha, \sin\theta_\alpha \sin\phi_\alpha, \cos\theta_\alpha), \tag{10}$$

$$\mathbf{x}_\beta = (\sin\theta_\beta \cos\phi_\beta, \sin\theta_\beta \sin\phi_\beta, \cos\theta_\beta), \tag{11}$$

in (7), the equations become:

$$\dot{\theta}_\alpha = -\frac{1}{2\pi} \sum_{\beta=1}^{N}{}' \frac{\Gamma_\beta \sin(\theta_\beta)\sin(\phi_\alpha - \phi_\beta)}{2(1-\cos(\gamma_{\alpha\beta}))}, \tag{12}$$

$$\sin(\theta_\alpha)\dot{\phi}_\alpha = \frac{1}{2\pi} \sum_{\beta=1}^{N}{}' \frac{\Gamma_\beta(\sin(\theta_\alpha)\cos(\theta_\beta) - \cos(\theta_\alpha)\sin(\theta_\beta)\cos(\phi_\alpha - \phi_\beta))}{2(1-\cos(\gamma_{\alpha\beta}))}, \tag{13}$$

where the denominator is the chord distance (squared) between vortex α and vortex β:

$$2(1-\cos(\gamma_{\alpha\beta})) = 2(\cos(\theta_\alpha)\cos(\theta_\beta) + \sin(\theta_\alpha)\sin(\theta_\beta)\cos(\phi_\alpha - \phi_\beta)) \equiv l_{\alpha\beta}^2. \tag{14}$$

These equations have a Hamiltonian structure, where

$$\mathcal{H} = -\frac{1}{4\pi} \sum_{\alpha<\beta} \Gamma_\alpha \Gamma_\beta \log(l_{\alpha\beta}^2) \tag{15}$$

is the logarithmic interaction energy, and the canonical variables are:

$$P_\alpha \equiv \sqrt{|\Gamma_\alpha|}\cos(\theta_\alpha); \quad Q_\alpha \equiv \sqrt{|\Gamma_\alpha|}\phi_\alpha. \tag{16}$$

This gives:

$$\dot{P}_\alpha = \frac{\partial \mathcal{H}}{\partial Q_\alpha}, \quad \dot{Q}_\alpha = -\frac{\partial \mathcal{H}}{\partial P_\alpha}. \tag{17}$$

Note that as in the planar problem, the position and momentum variables are the actual coordinates specifying the location of each vortex on the two-dimensional spherical surface and one of the conserved quantities is $\mathcal{H}$.

In addition to (15), there are other known conserved quantities associated with the three components of the center-of-vorticity vector, due to invariance of the system of particles under rotation around each of the axes. We write these components as (J_x, J_y, J_z) :

$$J_x = \sum_{\alpha=1}^{N} \Gamma_\alpha x_\alpha = \sum_{\alpha=1}^{N} \Gamma_\alpha \sin(\theta_\alpha)\cos(\phi_\alpha), \tag{18}$$

$$J_y = \sum_{\alpha=1}^{N} \Gamma_\alpha y_\alpha = \sum_{\alpha=1}^{N} \Gamma_\alpha \sin(\theta_\alpha)\sin(\phi_\alpha), \tag{19}$$

$$J_z = \sum_{\alpha=1}^{N} \Gamma_\alpha z_\alpha = \sum_{\alpha=1}^{N} \Gamma_\alpha \cos(\theta_\alpha), \tag{20}$$

and then define the *center-of-vorticity* vector as:

$$\mathbf{J} \equiv (J_x, J_y, J_z). \tag{21}$$

As a result of these conserved quantities, the system is integrable for $N \leq 3$, and when $\mathbf{J} = 0$, it is also integrable for $N = 4$, as was proven in Kidambi and Newton [18], Borisov and Pavlov [5], Borisov and Lebedev [6] and Sakajo [36,37]. The clean, integrable problem $N \leq 3$ is basically understood from the point of view of dynamics, and kinematic structure. Breaking symmetry about any axis generally breaks the conservation of **J** resulting in a loss of integrability. Natural geophysical mechanisms which accomplish this are described next.

2 Rotation, misalignment, and coupling

2.1 Misalignment of **J** vector

A more complex and interesting model is obtained by including solid-body rotation around the North-South polar axis [26], hence:

$$\dot{\mathbf{x}}_\alpha = \sum_{\beta=1}^{N}{}' \frac{\Gamma_\beta}{4\pi} \frac{\mathbf{x}_\beta \times \mathbf{x}_\alpha}{(1 - \mathbf{x}_\alpha \cdot \mathbf{x}_\beta)} + \Omega \hat{\mathbf{e}}_z \times \mathbf{x}_\alpha, \quad (\alpha = 1, \ldots, N) \tag{22}$$

$$\mathbf{x}_\alpha \in R^3, \quad \|\mathbf{x}_\alpha\| = 1. \tag{23}$$

Here, Ω is the solid-body angular frequency about $\hat{\mathbf{e}}_z$, which is aligned with the polar axis. The orientation of **J** with respect to this axis is crucial towards understanding subsequent motion of the system. We call (22) the 'one-way' coupled model [26], as the vortex motion is influenced by the solid-body rotation, but the solid-body field is not influenced by the point-vortices. As such, it is not a consistent discretization of the full Euler equations on the sphere as is (22) with $\Omega = 0$, but nonetheless we have found it to be a very convenient step towards deciphering the dynamics in a fully-coupled two-way approach [25].

As shown in Fig. 5, the importance of the misalignment is seen most clearly with a dipole configuration whose **J** vector is not aligned with the axis of rotation. A generic initial set-up is shown in Fig. 5a. The global motion can be viewed as a linear superposition of rotations around the **J** axis and the $\hat{e}_z$ axis, with corresponding frequencies ω and Ω. The resulting motion of the dipole depends on the relative orientations of the two axes, but two distinct global trajectories produced by the combination are shown in Figs. 5b, c. The first is the spherical analogue of Hobson's [15] 'tumbling mode' identified in β-plane studies of dipole motion, while the second is his 'wobbling mode'. More details and other configurations can be found in Newton and Shokraneh [26].

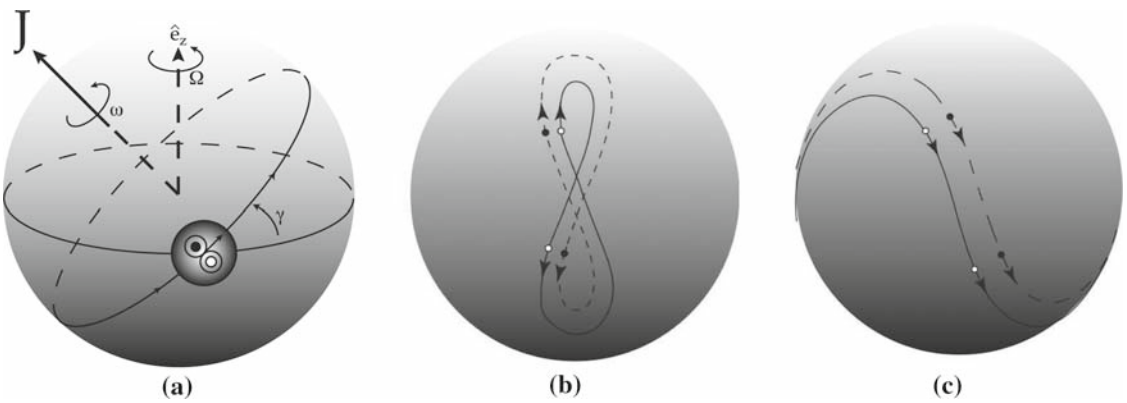

Fig. 5 **a** Dipole whose center-of-vorticity vector is misaligned with the axis of rotation creates trajectories that are linear combinations of rotations about two axes with two frequencies. **b** Global dipole tumbling mode that can be compared with Hobson's [15] β-plane tumbling mode. **c** Global dipole wobbling mode that can be compared with Hobson's [15] β-plane wobbling mode

2.2 Coupling of the $\mathbf{J}$ vectors

When more than one dipole is present, the system is a paradigm for the influence of global coupling between the local center-of-vorticity vectors as shown schematically in Fig. 2b in a more complex environment. For this, we assume $N = 2M$ in (22) where M is the number of dipoles. We group the point vortices in pairs $(\mathbf{x}_\alpha, \mathbf{x}_{\alpha+M})$, $(\alpha = 1, \ldots, M)$, with $\Gamma_{\alpha+M} = -\Gamma_\alpha$, where each pair represents a dipole. The nonlinear coupling is most cleanly seen by introducing a new set of dipole-based coordinates $(\mathbf{J}_\alpha, \mathbf{J}_{\alpha+M})$ which are derived from the original vortex coordinates $(\mathbf{x}_\alpha, \mathbf{x}_{\alpha+M})$ via the linear transformation

$$\mathbf{J}_\alpha \equiv \Gamma_\alpha(\mathbf{x}_\alpha - \mathbf{x}_{\alpha+M}) \tag{24}$$

$$\mathbf{J}_{\alpha+M} \equiv \Gamma_\alpha(\mathbf{x}_\alpha + \mathbf{x}_{\alpha+M}). \tag{25}$$

The vectors $\mathbf{J}_\alpha$ represent the centers-of-vorticity of each of the M dipoles, while $\mathbf{J}_{\alpha+M}$ are their centroids. In the new dipole coordinates, the full system of equations for the M-interacting dipoles become:

$$\begin{aligned}
\dot{\mathbf{J}}_\alpha = {} & \Omega\hat{e}_z \times \mathbf{J}_\alpha + \frac{\Gamma_\alpha}{4\pi} {\sum_{\beta=1}^{M}}' \Gamma_\beta \left\{ \frac{(\mathbf{J}_\beta + \mathbf{J}_{\beta+M}) \times (\mathbf{J}_\alpha + \mathbf{J}_{\alpha+M})}{4\Gamma_\alpha\Gamma_\beta - (\mathbf{J}_\alpha + \mathbf{J}_{\alpha+M}) \cdot (\mathbf{J}_\beta + \mathbf{J}_{\beta+M})} \right. \\
& - \frac{(\mathbf{J}_\beta - \mathbf{J}_{\beta+M}) \times (\mathbf{J}_\alpha + \mathbf{J}_{\alpha+M})}{4\Gamma_\alpha\Gamma_\beta + (\mathbf{J}_\alpha + \mathbf{J}_{\alpha+M}) \cdot (\mathbf{J}_\beta - \mathbf{J}_{\beta+M})} + \frac{(\mathbf{J}_\beta + \mathbf{J}_{\beta+M}) \times (\mathbf{J}_\alpha - \mathbf{J}_{\alpha+M})}{4\Gamma_\alpha\Gamma_\beta + (\mathbf{J}_\alpha - \mathbf{J}_{\alpha+M}) \cdot (\mathbf{J}_\beta + \mathbf{J}_{\beta+M})} \\
& \left. + \frac{(\mathbf{J}_\beta - \mathbf{J}_{\beta+M}) \times (\mathbf{J}_\alpha - \mathbf{J}_{\alpha+M})}{4\Gamma_\alpha\Gamma_\beta - (\mathbf{J}_\alpha - \mathbf{J}_{\alpha+M}) \cdot (\mathbf{J}_\beta - \mathbf{J}_{\beta+M})} \right\}
\end{aligned} \tag{26}$$

$$\begin{aligned}
\dot{\mathbf{J}}_{\alpha+M} = {} & \frac{1}{4\pi} \frac{\mathbf{J}_\alpha \times \mathbf{J}_{\alpha+M}}{1 + \frac{1}{4\Gamma_\alpha^2}(\|\mathbf{J}_\alpha\|^2 - \|\mathbf{J}_{\alpha+M}\|^2)} + \Omega\hat{e}_z \times \mathbf{J}_{\alpha+M} \\
& + \frac{\Gamma_\alpha}{4\pi} {\sum_{\beta=1}^{M}}' \Gamma_\beta \left\{ \frac{(\mathbf{J}_\beta + \mathbf{J}_{\beta+M}) \times (\mathbf{J}_\alpha + \mathbf{J}_{\alpha+M})}{4\Gamma_\alpha\Gamma_\beta - (\mathbf{J}_\alpha + \mathbf{J}_{\alpha+M}) \cdot (\mathbf{J}_\beta + \mathbf{J}_{\beta+M})} - \frac{(\mathbf{J}_\beta - \mathbf{J}_{\beta+M}) \times (\mathbf{J}_\alpha + \mathbf{J}_{\alpha+M})}{4\Gamma_\alpha\Gamma_\beta + (\mathbf{J}_\alpha + \mathbf{J}_{\alpha+M}) \cdot (\mathbf{J}_\beta - \mathbf{J}_{\beta+M})} \right. \\
& \left. - \frac{(\mathbf{J}_\beta + \mathbf{J}_{\beta+M}) \times (\mathbf{J}_\alpha - \mathbf{J}_{\alpha+M})}{4\Gamma_\alpha\Gamma_\beta + (\mathbf{J}_\alpha - \mathbf{J}_{\alpha+M}) \cdot (\mathbf{J}_\beta + \mathbf{J}_{\beta+M})} - \frac{(\mathbf{J}_\beta - \mathbf{J}_{\beta+M}) \times (\mathbf{J}_\alpha - \mathbf{J}_{\alpha+M})}{4\Gamma_\alpha\Gamma_\beta - (\mathbf{J}_\alpha - \mathbf{J}_{\alpha+M}) \cdot (\mathbf{J}_\beta - \mathbf{J}_{\beta+M})} \right\}
\end{aligned} \tag{27}$$

This system has many nice properties. Although $\mathbf{J}_\alpha \neq$ const., the total center-of-vorticity is conserved, i.e., $\sum_{\alpha=1}^{M} \mathbf{J}_\alpha =$ const. It can be shown that $\mathbf{J}_\alpha \perp \mathbf{J}_{\alpha+M}$. Also, if we isolate the first terms in (26), (27) by dropping the summations in both equations, the system reduces to those for an isolated dipole whose trajectories are shown in Fig. 5. We prove in Newton and Shokraneh [27] that these equations imply $\|\mathbf{J}_\alpha\| =$ const., $\|\mathbf{J}_{\alpha+M}\| = const.$, and that the intersection of $\mathbf{J}_{\alpha+M}$ with the surface of the sphere, when $\Omega = 0$, traces out a great circle (geodesic). The fully coupled system (26), (27) can be viewed as a system of billiards (geodesic motion) with long-range interactions causing the trajectories to deviate from geodesic flow.

2.3 How Rossby waves break integrability

A vortex ring configuration 'embedded' in a background vorticity field that mimicks solid body rotation is shown schematically in Fig. 6. To study how the background couples to the ring and breaks the conservation of $\mathbf{J}$ associated with it, we simultaneously track the point vortices constituting the ring along with a discretization of the contours separating the strips of constant vorticity regions of the background flow. Models of this type were developed by Dritschel and Polvani [11] then used in DiBattista and Polvani [10] to study dipole evolution, and Newton and Sakajo [25] to study the evolution of ring structures. The fully two-way coupled system that we use in Newton and Sakajo [25] is obtained from the regularized ($\delta > 0$) velocity field:

$$\begin{aligned}
\mathbf{u}_v^{(\delta)}(\mathbf{x}) &= \frac{\Gamma}{4\pi} \sum_{\alpha=1}^{N} \frac{\mathbf{x}_\alpha \times \mathbf{x}}{1 + \delta^2 - \mathbf{x} \cdot \mathbf{x}_\alpha}, \\
\mathbf{u}_s^{(\delta)}(\mathbf{x}) &= -\sum_{\alpha=1}^{M} \omega_\alpha \int_0^{2\pi} \log\left(|\mathbf{x} - \mathbf{X}_\alpha|^2 + \delta^2\right) \frac{\partial \mathbf{X}_\alpha}{\partial \theta} d\theta.
\end{aligned} \tag{28}$$

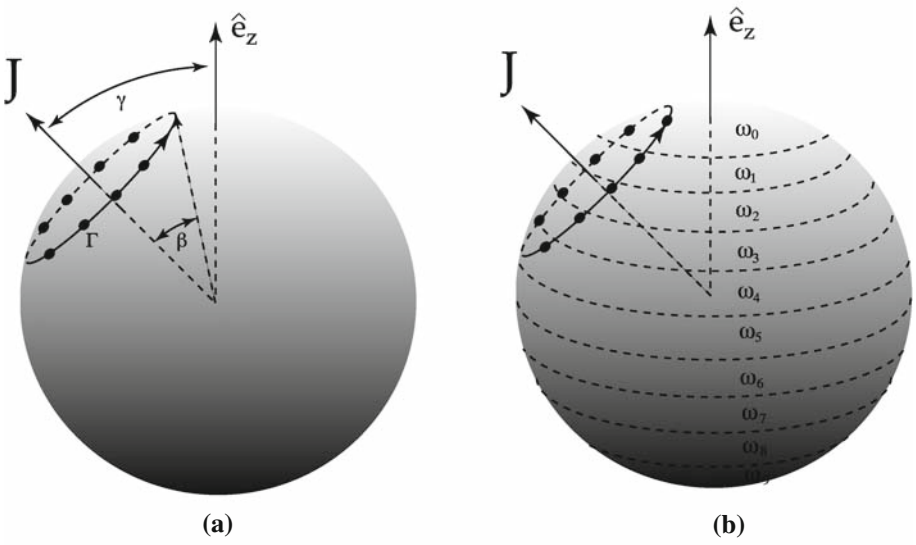

Fig. 6 The embedded dynamical system. Point vortices arranged in ring formation are embedded in a background field of continuous vorticity. The background field is made up of strips of constant vorticity whose strengths are chosen to represent solid-body rotation. The contours which separate the strips are discretized and tracked along with the point vortices making up the ring

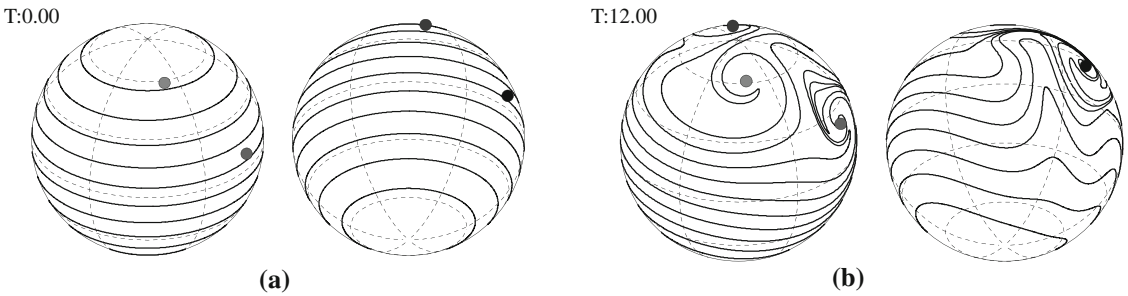

Fig. 7 **a** Initial orientation of four-point vortex ring embedded in a background field consisting of ten strips of constant vorticity. **b** Subsequent fully coupled evolution of the ring with the background. Note the wrapping of the vorticity strips around the point vortices effectively increasing their strength. See Newton and Sakajo [25] for full details

Here, $\mathbf{u}_v^{(\delta)}(\mathbf{x})$ represents the regularized velocity field due to each of the N equal strength (Γ) point vortices, while $\mathbf{u}_s^{(\delta)}(\mathbf{x})$ represents the velocity field generated by each constant vorticity strip (ω_α), whose contours are parametrized by $\mathbf{X}_\alpha$. When the contours are discretized, $\mathbf{X}_k$, $(k = 1, \ldots, M)$, one obtains a dynamical system of the form:

$$\frac{\partial \mathbf{x}_j}{\partial t} = \mathbf{u}_v^{(\delta)}(\mathbf{x}_j) + \mathbf{u}_s^{(\delta)}(\mathbf{x}_j), \quad j = 1, \ldots, N, \tag{29}$$

$$\frac{\partial \mathbf{X}_k}{\partial t} = \mathbf{u}_s^{(\delta)}(\mathbf{X}_k) + \mathbf{u}_v^{(\delta)}(\mathbf{X}_k), \quad k = 1, \ldots, M. \tag{30}$$

The fully coupled system evolves as shown in Fig. 7 for a ring comprised of four point vortices and ten constant vorticity strips. Note the wrapping of the contours around the point vortices effectively increases their strength relative to the background. In Newton and Sakajo [25] we show in detail how integrability is lost (for the ring) via the following clear sequence of events:

1. The ring triggers an instability in the background field and sets Rossby waves in motion.
2. These waves, which move retrograde to the solid-body rotation (as pointed out in [10]), cause the ring to alter its initial rotational direction.
3. The wrapping of contours around point vortices effectively increases the strength of the ring.
4. Eventually, the point vortices are strong enough to overcome the effect of the Rossby waves, thus the ring reverts back to its original rotational direction.

5. Energy is continually exchanged between the ring and the background field breaking the conservation of both H and $\mathbf{J}$ (associated with the ring).
6. The stability and integrity of the ring is compromised.

The long-time evolution of the N-vortices constituting the ring are expected to be chaotic, although there are significant computational challenges for producing accurate long-time measures of nonintegrability (e.g., Lyapunov exponents) due to the need to accurately track the contours whose length grows continuously requiring frequent re-meshing.

3 Polar vortex splitting event

A nice paradigm for studying global transport on the sphere due to a 'local' geophysical event is the much studied Polar vortex splitting event of 2002. The event is thoroughly documented in a devoted journal issue—*Journal of Atmospheric Sciences*: Special Issue on the Antarctic Stratospheric Sudden Warming and Split Ozone Hole of 2002, 62(3) March 2005.

In late September of 2002, over a period of a few days, the Antarctic ozone hole split in two. This is clearly evident in the ozone concentrations shown in Fig. 8. A split ozone hole implies a split vortex which subsequently initiated a sudden stratospheric warming. These types of warmings occur on a regular basis in the Arctic (although not annually) and are thought to be produced by the dynamical momentum forcing resulting from the breaking and dissipation of planetary-scale Rossby waves in the stratosphere. Prior to 2002, however, no stratospheric sudden warming had been observed in the Antarctic, and it was widely believed to be impossible. Figure 8 shows three panels of the Antarctic ozone hole in September 2001 (one year before the split), September 2002 (split ozone hole), and September 2003 (one year after the split). The goal of modeling such an event are first, to capture the basic features of this complex vortex splitting process, then to use a simple model to analyze its effect on the global transport of atmospheric tracer particles.

The ingredients for the model can be captured, most simply, in a linear setting. We imagine that the Polar vortex is a passive patch being pulled and stretched at the Pole by a perturbed ring configuration representing the outer edge (shear layer) of the vortex, as shown initially in Fig. 10a. Since the Polar patch is centered at an elliptic point generated by the point vortices, one might first consider a linearized problem around the Pole. First, we construct a time-dependent Hamiltonian system with a fixed point (the center of the Polar vortex) that oscillates between hyperbolic and elliptic through one period:

$$\mathcal{H}(x, y; t) = \frac{1}{2}a(t)x^2 + \frac{1}{2}b(t)y^2, \tag{31}$$

hence

$$\dot{\mathbf{x}} = A\mathbf{x}; \quad \mathbf{x} = \begin{pmatrix} x \\ y \end{pmatrix}; \quad A = \begin{pmatrix} 0 & b(t) \\ -a(t) & 0 \end{pmatrix}. \tag{32}$$

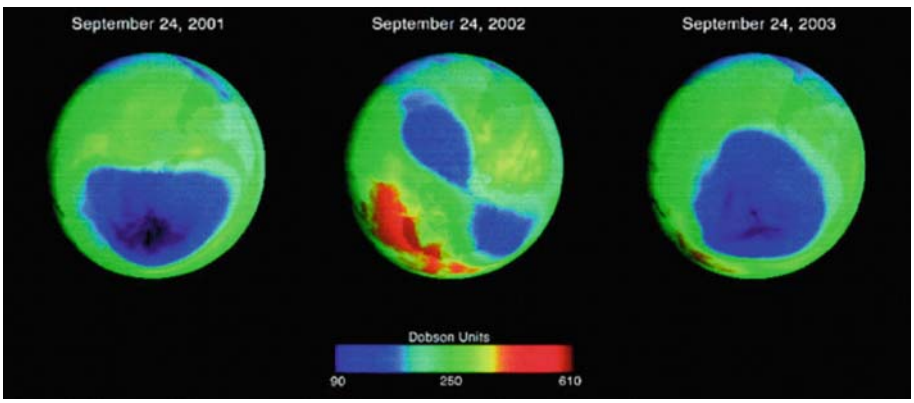

Fig. 8 The splitting of the Antarctic ozone hole (http://www.gse-promote.org/), September 2002, as evident in total column ozone concentration. September 2001 and September 2003 are shown for comparison. The splitting event in 2002 is also evident in the stratospheric vorticity or potential vorticity fields

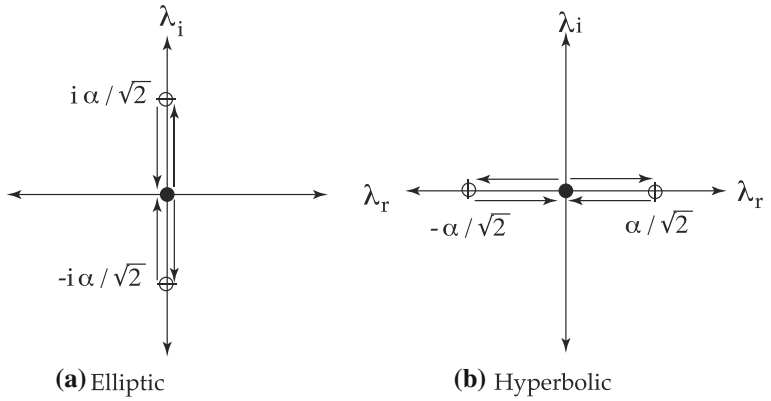

Fig. 9 Eigenvalue evolution of the time-dependent matrix **A** through one period as a linear mechanism capable of pinching off a passive patch. **a** First half period $0 \le t \le \pi/\omega$ in which the eigenvalues lie on the imaginary axis; **b** Second half period $\pi/\omega \le t \le 2\pi/\omega$ in which they lie on the real axis

The instantaneous eigenvalues of A are $\lambda = \pm\sqrt{-ab}$, where we let:

$$a(t) = \alpha \sin(\omega t/2), \tag{33}$$
$$b(t) = \alpha \cos(\omega t/2), \tag{34}$$

so that $\lambda(t) = \pm\frac{\alpha}{\sqrt{2}}\sqrt{-\sin(\omega t)}$. The evolution of the eigenvalues, through one period, is shown in Fig. 9. For half the period, the hyperbolic structure elongates and begins to tear the patch apart, whereas for the other half period, the elliptic structure rotates and wraps the patch on itself. We further transform coordinates to a rotating frame by letting:

$$\mathbf{x}_r = M\mathbf{x}, \tag{35}$$

where

$$M = \begin{pmatrix} \cos\Omega t & -\sin\Omega t \\ \sin\Omega t & \cos\Omega t \end{pmatrix}, \quad \mathbf{x}_r = \begin{pmatrix} x_r \\ y_r \end{pmatrix}. \tag{36}$$

Then $\dot{\mathbf{x}} = \dot{M}^T\mathbf{x}_r + M^T\dot{\mathbf{x}}_r$, where $M^{-1} \equiv M^T$. In the new coordinates, this gives rise to the time-dependent Hamiltonian:

$$\begin{aligned}\mathcal{H}(x_r, y_r; t) = &\frac{1}{2}(b(t)\sin^2\Omega t + a(t)\cos^2\Omega t - \Omega)x_r^2 + (a(t) - b(t))\cos\Omega t \sin\Omega t x_r y_r \\ &+\frac{1}{2}(a(t)\sin^2\Omega t + b(t)\cos^2\Omega t - \Omega)y_r^2.\end{aligned} \tag{37}$$

To see the effect of such a construction in a full nonlinear setting, we focus on a perturbed vortex ring formation. The outer edge of the polar vortex constitutes a shear layer, as represented in our model by the initial placement of point vortices while their subsequent evolution represents the deformation of the Polar vortex region. A prototypical splitting event can be created by a perturbed latitudinal 4-vortex ring, when the perturbation amplitude (a sub-harmonic perturbation in which the initial position of every other vortex is shifted by a small amount in order to initiate the pairing process) exceeds a certain threshold. The grey patch in the middle region of the ring shown in Fig. 10 pinches in the middle to form two elliptic regions, which subsequently stretch and fold due to a blinking back and forth between a local elliptic region and a hyperbolic region created by the perturbed ring. Measures of ergodicity and transport of these kinds of perturbed ring models and the connection with topological bifurcations of global streamline patterns can be found in Newton and Ross [24].

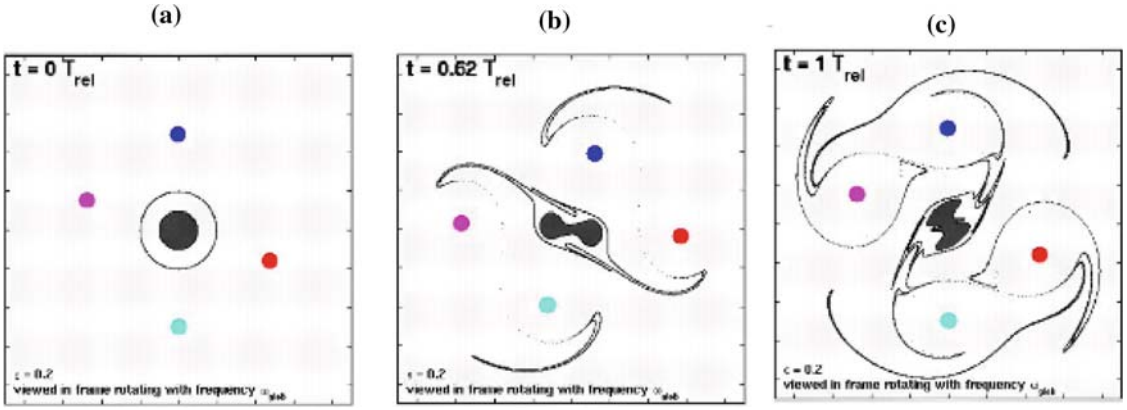

Fig. 10 A perturbed four-vortex ring demonstrating its ability to split a single passive patch into two. The streamlines blink back and forth between and elliptic region and a hyperbolic region which is ultimately responsible for the stretching and pinch-off of the passive mass

4 Extensions and discussion

We finish by pointing to two important extensions to the current hierarchy of models described in the paper that are key extensions from the point of view of understanding and modeling atmospheric dynamics. Both of these, alone, would break the integrability of the basic model for $N = 3$ by destroying the underlying conserved quantities. First, one must conserve *potential vorticity* Q, defined as:

$$Q = \left(\frac{\omega + f}{H}\right) = \text{const.}, \tag{38}$$

where $\omega = \sum_{\alpha=1}^{N} \Gamma_\alpha$, $f = 2\Omega_p \sin\phi$ (Coriolis term), and $H = 1$ (layer depth). To achieve this, one can allow the point-vortex intensities Γ_α to depend on position ϕ_α:

$$\Gamma_\alpha(\phi_\alpha) + 2\Omega_p \sin\phi_\alpha = \Gamma_\alpha^{(0)} + 2\Omega_p \sin\phi_\alpha^{(0)}, \tag{39}$$

where $\Gamma_\alpha^{(0)}$ and $\phi_\alpha^{(0)}$ represents their intensity and position initially. The vortex intensity as a function of position is then given as:

$$\Gamma_\alpha(\phi_\alpha) = 2\Omega_p(-\sin\phi_\alpha + \sin\phi_\alpha^{(0)}) + \Gamma_\alpha^{(0)}. \tag{40}$$

With the center-of-vorticity vector defined as in (24), clearly we lose these important conserved quantities and it is hard to imagine how integrability is maintained, or even relevant.

Second, because of uncertainty in data measurements as well as incomplete modeling assumptions, it is desirable to construct a probabilistic version of the models presented in this paper. A natural way to achieve this is shown in Fig. 11. Instead of working with the deterministic point-vortex positions, one should work with the equations that govern their probability density functions (pdf's). In isolation, as shown in Fig. 11a, the pdf associated with an individual point-vortex is the solution to the heat-equation on the surface of a sphere, hence the probabilistic 'position' (i.e., the 'support' of the probability density function) of the point-vortex diffuses self-similarly until in the limit $t \longrightarrow \infty$, it is equally likely to be located anywhere on the sphere's surface. However, since the collection of point-vortices interact nonlinearly according to the evolution equations (7), we replace the deterministic position variables, $\mathbf{x}_\alpha$ in this formulation with the mean value $\boldsymbol{\mu}_\alpha$. The probability density function for each point-vortex would then be governed (approximately) by:

$$p(\mathbf{s}_\alpha, t; \boldsymbol{\mu}_\alpha) \sim \frac{1}{4\pi D t} \exp(-|\mathbf{s}_\alpha - \boldsymbol{\mu}_\alpha|^2/4Dt), \tag{41}$$

where $\boldsymbol{\mu}_\alpha$ is governed by the system (7). Here $\mathbf{s}_\alpha$ is the *geodesic* distance from the mean $\boldsymbol{\mu}_\alpha$, and D is a diffusion constant related to the time-scale at which uncertainty infiltrates the deterministic system. Thus, the full system will unfold dynamically carrying a mixture of a 'deterministic' timescale (say, the positive Lyapunov exponents in the case $N > 3$) associated with the basic model (22) along with a timescale associated with

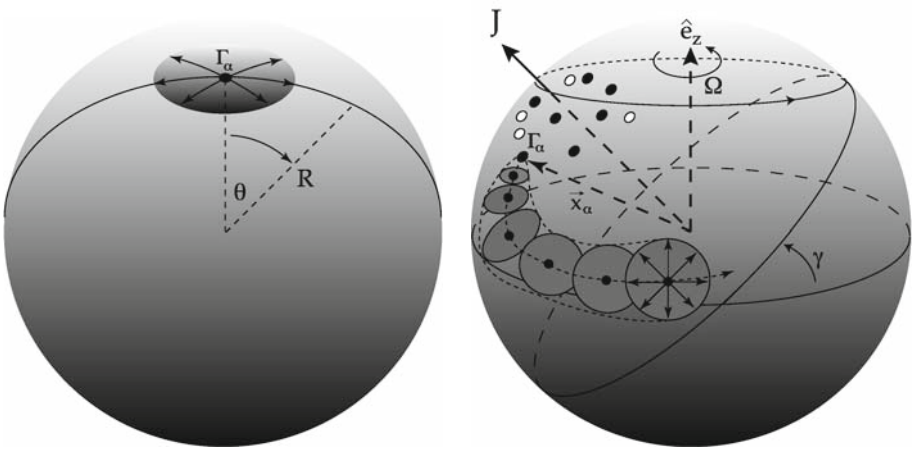

Fig. 11 **a** The support of the probability density function associated with an isolated point-vortex on a sphere of radius R grows self-similarly according to the diffusion equation on the surface of a sphere. **b** In addition, the collection of point-vortices interact according to the N-vortex dynamical system (7). The combination of these two effects remain to be explored

the rate at which uncertainty pervades the system (i.e., the diffusion constant D). The future development of any initial configuration intended to model a specific atmospheric event must depend on the interplay of these important timescales. Extensions such as these remain to be developed further within the context of the models presented in this paper.

Low dimensional and 'embedded' models of specific atmospheric events, of the type discussed in this article, offer the possibility of obtaining detailed quantitative results in simplified settings based on analysis and simulation which ultimately can be validated or invalidated with more realistic numerical models and atmospheric data. The emphasis here has been on pointing out the importance of (i) the misalignment of the **J** vector with the axis of rotation; (ii) coupling with the background field which, at the very least, means full nonlinear interaction with Rossby waves; (iii) periodic oscillation of the local eigenvalue structure from hyperbolic to elliptic as a linear mechanism capable of splitting and stretching a passive patch; (iv) subsequent deformation and transport of the patch due to finite-amplitude oscillations of the shear layer constituting the outer layer of the Polar vortex. Within the context of these models, potential vorticity conservation and probabilistic ingredients are currently being developed.

Acknowledgments Funding for this work was provided by the National Science Foundation through grants NSF-DMS-0504308 and NSF-DMS-0804629. I would like to thank R. Kidambi, M. Jamaloodeen, H. Shokraneh, and G. Chamoun whose Ph.D. theses, along with the postdoctoral work of Shane Ross at USC helped develop aspects of what is described in this article. I would also like to thank colleagues from whom I have learned much including Hassan Aref, Alexey Borisov, Darren Crowdy, David Dritschel, Eva Kanso, Yoshi Kimura, Chjan Lim, Phil Marcus, Jerry Marsden, Takashi Sakajo, Mark Stremler and Tamas Tel.

References

1. Baines, P.: The stability of planetary waves on a sphere. J. Fluid Mech. **73**, 193–213 (1976)
2. Boatto, S., Pierrehumbert, R.T.: Dynamics of a passive scalar in a velocity field of four identical point vortices. J. Fluid Mech. **394**, 137–174 (1999)
3. Bogomolov, V.A.: Two-dimensional fluid dynamics on a sphere. Izv. Atm. Ocean. Phys. **15**(1), 18–22 (1979)
4. Bogomolov, V.A.: Dynamics of vorticity at a sphere. Fluid Dyn. **6**, 863–870 (1977)
5. Borisov, A.V., Pavlov, A.E.: Dynamics and statics of vortices on a plane and a sphere I. Regul. Chaotic Dyn. **3**(1), 28–38 (1998)
6. Borisov, A.V., Lebedev, V.G.: Dynamics and statics of vortices on a plane and a sphere II. Regul. Chaotic Dyn. **3**(2), 99–114 (1998)
7. Bowman, K.P., Mangus, N.J.: Observations of deformation and mixing of the total ozone field in the antarctic polar vortex. J. Atmos. Sci. **50**(17), 2915–2921 (1993)
8. Charlton, A.J., O'Neil, A., Lahoz, W.A., Berrisford, P.: The splitting of the stratospheric polar vortex in the southern hemisphere, September 2002: Dynamical evolution. J. Atmos. Sci. **62**, 590–602 (2005)
9. Cushman-Roisin, B.: Introduction to Geophysical Fluid Dynamics. Prentice-Hall, NJ (1994)
10. DiBattista, M.T., Polvani, L.M.: Barotropic vortex pairs on a rotating sphere. J. Fluid Mech. **358**, 107–133 (1998)

11. Dritschel, D.G., Polvani, L.M.: The roll-up of vorticity strips on the surface of a sphere. J. Fluid Mech. **234**, 47–69 (1992)
12. Haynes, P.: Transport, stirring and mixing in the atmosphere. In: Chaté, H., Villermaux, E. (eds.) Proceedings of the NATO Advanced Study Institute on Mixing, Chaos and Turblence, Cargese Corse, France, 7–20 July 1996, pp. 229–272. Kluwer, Dordrecht (1999)
13. Haynes, P.: Stratospheric dynamics. Ann. Rev. Fluid Mech. **37**, 263–293 (2005)
14. Helmholtz, H.: On integrals of the hydrodynamical equations, which express vortex-motion. Phil. Mag. (Ser. 4) **33**, 485–510 (1858)
15. Hobson, D.D.: A point vortex dipole model of an isolated modon. Phys. Fluids A **3**, 3027–3033 (1991)
16. Joseph, B., Legras, B.: Relation between kinematic boundaries, stirring, and barriers for the Antarctic polar vortex. J. Atmos. Sci. **59**, 1198–1212 (2002)
17. Katok, A., Hasselblatt, B.: Introduction to the Modern Theory of Dynamical Systems. Cambridge University Press, London (1995)
18. Kidambi, R., Newton, P.K.: Motion of three point vortices on a sphere. Physica D **116**, 143–175 (1998)
19. Kidambi, R., Newton, P.K.: Streamline topologies for integrable vortex motion on a sphere. Physica D **140**, 95–125 (2000)
20. Marcus, P.S.: Jupiter's Great Red Spot and other vortices. Ann. Rev. Astron. Astrophys. **31**, 523–573 (1993)
21. McDonald, N.R.: The time-dependent behavior of a spinning disc on a rotating planet: a model for geophysical vortex motion. Geo. Astro. Fluid Dyn. **87**, 253–272 (1998)
22. McDonald, N.R.: The motion of geophysical vortices. Phil. Trans. R. Soc. Lond. A **357**, 3427–3444 (1999)
23. Newton, P.K.: The N-vortex problem: analytical techniques. In: Applied Mathematical Science, vol. 145. Springer, New York (2001)
24. Newton, P.K., Ross, S.D.: Chaotic advection in the restricted four-vortex problem on a sphere. Physica D (1) **223**, 36–53 (2006)
25. Newton, P.K., Sakajo, T.: The N-vortex problem on a rotating sphere: III. Ring configurations coupled to a background field. Proc. R. Soc. A **463**, 961–977 (2007)
26. Newton, P.K., Shokraneh, H.: The N-vortex problem on a rotating sphere: I multi-frequency configurations. Proc. R. Soc. A **462**, 149–169 (2006)
27. Newton, P.K., Shokraneh, H.: Interacting dipole pairs on a rotating sphere. Proc. R. Soc. A **464**(2094), 1525–1541 (2008)
28. Nycander, J.: Analogy between the drift of planetary vortices and the precession of a spinning body. Plasma Phys. Rep. **22**, 771–774 (1996)
29. Pierrehumbert, R.T.: Chaotic mixing of tracer and vorticity by modulated travelling Rossby waves. Geo. Astro. Fluid. Dyn. **58**, 285–319 (1991)
30. Pierrehumbert, R.T., Yang, H.: Global chaotic mixing on isentropic surfaces. J. Atmos. Sci. **50**(15), 2462–2480 (1993)
31. Polvani, L.M., Dritschel, D.G.: Wave and vortex dynamics on the surface of a sphere. J. Fluid Mech. **255**, 35–64 (1993)
32. Ripa, P.: Inertial oscillations and the β-plane approximation(s). J. Phys. Oceanogr. **27**, 633–647 (1997)
33. Ripa, P.: Effect of the Earth's curvature on the dynamics of isolated objects Part I: the disk. J. Phys. Oceanogr. **30**, 2072–2087 (2000)
34. Ripa, P.: Effect of the Earth's curvature on the dynamics of isolated objects Part II: the uniformly translating vortex. J. Phys. Oceanogr. **30**, 2504–2514 (2000)
35. Saffman, P.G.: Vortex Dynamics. Cambridge Monographs on Mechanics and Applied Mathematics. Cambridge University Press, London (1992)
36. Sakajo, T.: The motion of three point vortices on a sphere. Jpn. J. Ind. Appl. Math. **16**, 321–347 (1999)
37. Sakajo, T.: Integrable four-vortex motion on a sphere with zero moment of vorticity. Phys. Fluids **19**(1), 017109 (2007)
38. Simmons, A., Mortal, M., Kelly, G., McNally, A., Untch, A., Uppala, S.: ECMWF analysis and forecasts of stratospheric winter polar vortex break-up: September 2002 in the southern hemisphere and related events. J. Atmos. Sci. **62** (2005)
39. Waugh, D.W.: Contour surgery simulations of a forced polar vortex. J. Atmos. Sci. **50**, 714–730 (1992)
40. Waugh, D.W., Plumb, R.A., Atkinson, R.J., Schoeberl, M.R., Lait, L.R., Newman, P.A., Loewenstein, M., Tooney, D.W., Avallone, L.M., Webster, C.R., May, R.D.: Transport out of the lower stratospheric Arctic vortex by Rossby wave breaking. J. Geo. Res. **99**(D1), 1071–1088 (1994)